Toxicology 260 (2009) 37–46

Contents lists available at ScienceDirect

Toxicology

journal homepage: www.elsevier.com/locate/toxicol

Induction of chronic inflammation in mice treated with titanium dioxide nanoparticles by intratracheal instillation

Eun-Jung Park[a], Junheon Yoon[b], Kyunghee Choi[b,**], Jongheop Yi[c], Kwangsik Park[a,*]

[a] College of Pharmacy, Dongduk Women's University, 23-1, Wolgok-dong, Seongbuk-gu, Seoul 136-714, Republic of Korea
[b] Department of Chemical Assessment, National Institute of Environmental Research, Kyungseo-dong, Seo-gu, Incheon 404-708, Republic of Korea
[c] School of Chemical and Biological Engineering, Seoul National University, 599 Gwanangno, Gwanak-gu, Seoul 151-742, Republic of Korea

ARTICLE INFO

Article history:
Received 17 January 2009
Received in revised form 28 February 2009
Accepted 6 March 2009
Available online 20 March 2009

Keywords:
Titanium dioxide nanoparticles
Cytokines
Granuloma
Chronic inflammation

ABSTRACT

Titanium dioxide nanoparticles (TNP) are nanomaterials which have various applications including photocatalysts, cosmetics, and pharmaceuticals because of their high stability, anticorrosiveness, and photocatalytic properties. Induction of cytokines and potential chronic inflammation were investigated in mice treated with TNP (5 mg/kg, 20 mg/kg, and 50 mg/kg) by a single intratracheal instillation. Pro-inflammatory cytokines such as IL-1, TNF-a, and IL-6 were significantly induced in a dose-dependent manner at day 1 after instillation. The levels of Th1-type cytokines (IL-12 and IFN-γ) and Th2-type cytokines (IL4, IL-5 and IL-10) were also elevated dose-dependently at day 1 and the inflammatory responses were sustained until the remainder of experimental period for 14 days. By the induction of Th2-type cytokines, the increased B cell distributions both in spleen and in blood, and increased IgE production in BAL fluid and serum were observed. In lung tissue, increase of inflammatory proteins (MIP and MCP) and granuloma formation were observed. Furthermore, the expressions of genes related with antigen presentation (H2-T23, H2-T17, H2-K1, and H2-Eb1) and genes related with the induction of chemotaxis of immune cells (Ccl7, Ccl3, Cxcl1, Ccl4, Ccl2) were markedly increased using microarray analysis. From these data, it could be suggested that TNP possibly cause chronic inflammatory diseases through Th2-mediated pathway in mice.

1. Introduction

With the increased application of nanomaterials, the discharge to environment through production, transportation, storage, and consumption process could be rapidly increased and it may exhibit adverse effects to human health. When inhaled, nanoparticles are efficiently deposited into lung cells. Translocation through epithelial and endothelial cells into the blood and lymph circulation may be occurred to reach potentially sensitive target sites including bone marrow, lymph nodes, spleen, and heart. Endocytosis and biokinetics of nanoparticles are largely dependent on nanoparticle surface chemistry and in vivo surface modifications (Oberdörster et al., 2005).

Titanium dioxide nanoparticles (TNP) have been widely used as a white pigment in paint, food colorant, ultraviolet blocker in cosmetics, welding rod-coating material, disinfectant in environment and wastewater, and photosensitizer for photodynamic therapy (Gurr et al., 2005). In 2006, IARC (International agency for research on cancer) classified pigment-grade titanium dioxide as group 2B carcinogen (possible to human). OECD Steering Group for Test Guidelines released the nanoparticle list of high priority and TNP was included in the list with fullerene, single-walled carbon nanotubes (SWCNTs), multi-walled carbon nanotubes (MWCNTs), silver nanoparticles, and others.

By epidemiological study, it was reported that a papillary adenocarcinoma was located in the lung of the 53-year-old male, who was engaged in packing titanium dioxide for about 13 years, and titanium was diffusely deposited in the lung and was engulfed by macrophages in the interstitium and alveolar spaces. Slight fibrosis of the interstitium around bronchioles and vessels was also observed (Yamadori et al., 1986). In animal study, exposure of titanium dioxide for 2 years to rats by inhalation revealed a dose-dependent dust cell accumulation, a foamy macrophage response, type II pneumocyte hyperplasia, alveolar proteinosis, alveolar bronchiolarization, cholesterol granulomas, focal pleurisy, bronchioloalveolar adenomas and cystic keratinizing squamous cell carcinomas (Lee et al., 1985).

Regarding the toxicity of nano-sized titanium dioxide particles, lungs showed significant changes in morphology and histology including disruption of the alveolar septa, alveolar enlargement (emphysematous change), type II pneumocyte proliferation, increased alveolar epithelial thickness, and the accumulation of particle-laden macrophages by a single instillation of TNP (Chen

* Corresponding author. Tel.: +82 32 560 7213; fax: +82 32 568 2041.
** Co-corresponding author. Tel: +82 2 940 4522; fax: +82 2 940 4159.
E-mail addresses: nierchoi@me.go.kr (K. Choi), kspark@dongduk.ac.kr (K. Park).

0300-483X/$ – see front matter © 2009 Elsevier Ireland Ltd. All rights reserved.
doi:10.1016/j.tox.2009.03.005

et al., 2006). By the inhalation, total cell number as well as the number of macrophages were found to be significantly increased in the BAL (Bronchoalveolar lavage) fluid collected from the treated mice (Grassian et al., 2007). Exposure to TNP could produce cytotoxicity, oxidative stress, lung inflammation, cell proliferation, and histopathological responses, with differential pulmonary effects (Warheit et al., 2007; Park et al., 2008; Reeves et al., 2008; Kang et al., 2008; Driscoll and Maurer, 1991). TNP increased the production of hydrogen peroxide and nitric oxide in human bronchial epithelial cells (Gurr et al., 2005) and also caused micronuclei formation and apoptosis in Syrian hamster embryo fibroblasts (Rahman et al., 2002).

There are many evidences that airborne particulate matter is an important factor associated with the enhanced prevalence of respiratory allergy (Haar et al., 2006: Alberg et al., 2009). In the reports, particulate matter showed allergy adjuvant activity measured as the production of ovalbumin-specific immunoglobulin (Ig)E. However, the effects of engineered nanoparticles on the potential allergic responses or chronic inflammation through B cell activation and IgE production have not been fully investigated. In this study, the induction of Th2-type cytokines, B cell activation, IgE production granuloma formation, and the expression of inflammation-related genes were investigated for potential chronic inflammatory diseases caused by TNP.

2. Materials and methods

2.1. Animals and titanium dioxide nanoparticles

ICR mice were purchased from Orient-Bio Animal Company (Seongnam, Korea) and were allowed to adapt to the animal room condition prior to initiation of the study. The environmental conditions were a temperature of $23 \pm 1\,^{\circ}C$; relative humidity of $55 \pm 5\%$; and a 12 h light/dark cycle. Commercial titanium dioxide nanoparticles (P-25, 21 nm-size) were purchased from Degussa Korea (Incheon, Korea). According to the information provided by the supplier, titanium dioxide P-25 is a fine white powder with hydrophilic character caused by hydroxyl groups on the surface (ca. 5 OH-groups/nm^2). It consists of aggregated primary particles. The aggregates are several hundred nanometre in size and the primary particles have a mean diameter of approximately 20 nm. Particle size and density of ca. 4 g/cm^3 lead to a specific surface of approximately 50 m^2/g. In some liquid phase application, the granulation of the powder may lead to particles with a mean diameter of micrometer level. In this study, TNP was suspended in phosphate buffered saline (PBS), and was sonicated prior to use to ensure a uniform suspension. TEM image of TNP suspension used for intratracheal instillation was made using transmission electron microscope (JEM1010, JEL, Japan) (Fig. 1A). Size-distribution of TNP suspension which was used for intratracheal instillation, was also analysed using particle sizing system (NICOMP, Santa Babara, CA, USA) and shown in Fig. 1B. The mean diameter of the agglomerated particles was about 200 nm. TNP was delivered with a 24-G catheter, at doses of 5, 20 or 50 mg/kg, by intratracheal instillation under light tiletamine anesthesia (Day 0). Then, the animals were sacrificed at 1, 7, 14 days after treatment ($n = 10$–12 per group).

2.2. Preparation of samples

At the selected time intervals after TNP treatment, blood was collected from the retro-orbital venous plexus using heparinized capillary tubes. Serum was obtained by centrifugation at 3000 rpm for 20 min. BAL fluid collection was performed by cannulating the trachea and lavaging the lungs with 1 ml of cold sterile Ca^{2+}/Mg^{2+} free PBS. Approximately 500–600 μl BAL fluid per mouse was harvested. Each BAL fluid was pooled and centrifuged at 3000 rpm for 10 min prior to measurement of cytokines. For the isolation of splenocytes, the spleen was aseptically removed from ICR mouse, and suspended by passage through sterile plastic strainer in Dulbecco's Modified Eagle's Medium (DMEM) with 2% fetal bovine serum (FBS). After centrifugation at 1500 rpm for 3 min, the supernatant was removed, and the pellet was briefly vortexed in 500 μl distilled water, then re-suspended in DMEM with 2% FBS. The cells were filtered through nylon mesh to yield the final splenocyte preparation (Byun et al., 2006; Vendrame et al., 2006; Manosroi et al., 2005; Cho et al., 2007).

2.3. Serum biochemistry and cytokine measurement

The levels of total protein (TP), albumin (ALB), aspartate aminotransferase (AST), alanine aminotransferase (ALT), alkaline phosphatase (ALP), r-glutamyl transferase (r-GT), creatinine, blood urea nitrogen (BUN), and cholesterol were determined using an automatic serum chemical analyzer (Shimadzu CL-7200, Shimadzu Co., Japan).

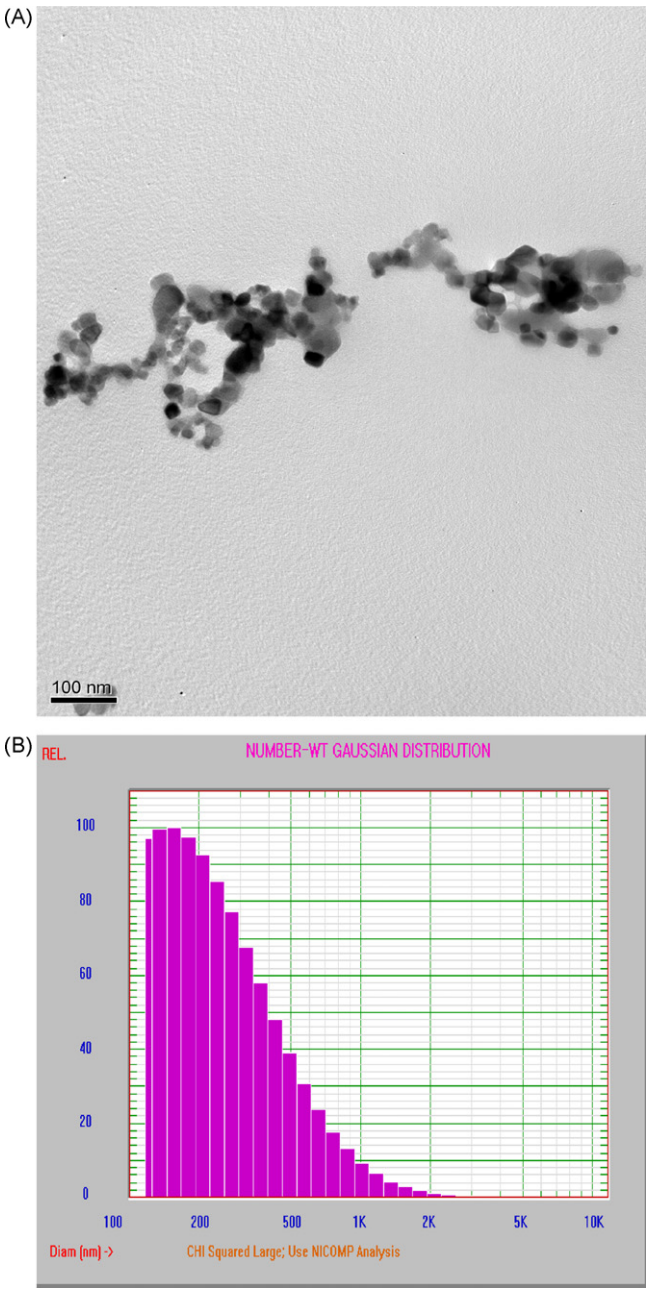

Fig. 1. TEM photograph and size-distribution of TNP preparation in PBS for intratracheal instillation. TNP was suspended 15 mg/ml in PBS, which is the same preparation used for the instillation dose of 50 mg/kg. TEM image (A) and size-distribution profile (B) were made after sonication.

The concentrations of each cytokine in the serum and in the supernatant of BAL fluid were determined using commercially available ELISA kits (eBioscience, San Diego, CA, USA). Briefly, each well of a microplate was coated with 100 μl of capture antibody, and incubated overnight at 4 °C. After washing and blocking with assay diluent, BAL fluid, serum or standard cytokines were added to individual wells and the plates were maintained for 2 h at room temperature. The plates were washed, then biotin-conjugated detecting mouse antibody was added to each well and incubated at room temperature for 1 h. The plates were washed again and further incubated with avidin–HRP for 30 min before detection with TMB solution. Finally, reactions were stopped by adding 1 M H_3PO_4, and absorbance at 450 nm was measured with an ELISA reader (Molecular Devices, Sunnyvale, CA, USA). The amount of cytokine was calculated from the linear portion of the generated standard curve (Byun et al., 2006).

2.4. Immunophenotyping of splenocytes

All monoclonal antibodies were purchased from eBioscience (San Diego, CA, USA), and T cells (CD3, 1:50), B cells (CD19, 1:50), NK cells (DX5, 1:100), $CD4^+$ T

cells ($CD4^+$, 1:160), and $CD8^+$ T cells ($CD8^+$, 1:50) were identified using directly conjugated anti-mouse antibody. Briefly, splenocytes of $3\sim5 \times 10^3$ and serum were blocked with Fc-block (eBioscience, San diego, CA, USA) to reduce non-specific antibody binding. Cells were then incubated in the dark with 10 μl of the appropriate fluorochrome-conjugated antibody for 20 min at 4 °C. Cells were washed with 500 μl FACS (Fluorescence Activated Cell Sorter) buffer. The blood was lysed for 5 min with FACS lysis buffer (BD Bioscience, Franklin Lakes, NJ, USA) at room temperature, then re-washed with FACS buffer. Finally, each sample was fixed with 1% paraformaldehyde until further analysis. Flow cytometry analysis was performed on the FACSCalibur system (BD Biosciences, Franklin Lakes, NJ, USA). Control samples were matched for each fluorochrome. Data were analysed using CellQuest software (Becton Dickinson, Franklin Lakes, NJ, USA) (Vendrame et al., 2006; Silva et al., 2005).

2.5. Measurement of IgE

The concentration of IgE in the serum and in the supernatant of BAL fluid was determined using commercially available IgE ELISA kits (Komabiotech, Seoul, Korea). Briefly, each well of microplates was coated with coating antibody and incubated overnight at 4 °C. After washing and blocking with blocking solution for 1 h at room temperature, BAL fluid, serum and IgE standard were added to individual wells and left for 1 h at room temperature. The plates were then washed, detection antibody was added to each well and the plates were incubated at room temperature for 1 h. After washing, the plates were further incubated with color development solution. Finally, the reaction was stopped by adding 2 M H_2SO_4, and absorbance at 450 nm was measured with an ELISA reader (Molecular Devices, Sunnyvale, CA, USA). The amounts of secreted IgE were calculated from the linear portion of the prepared standard curve (Ohrui et al., 2000).

2.6. Histopathology and immunohistochemistry

Lungs from each mouse were fixed with 10% neutral buffered formalin and processed using routine histological techniques. After paraffin embedding, 3 μm sections were cut and stained with hematoxylin and eosin (H&E) for histopathological evaluations. Paraffin-embedded sections of lung were used for the immunohistochemical detection of MCP-1 and MIP-2 (R & D System, Minneapolis, MN, USA). For the immunohistochemistry, the sections were mounted on silanized slides (Dako, Glostrup, Denmark), deparaffinized and rehydrated with a xylene–alcohol series to distilled water. The endogenous peroxidase activity was quenched with 3% hydrogen peroxide–methanol (1:1 vol/vol) solution at room temperature for 20 min. For antigen retrieval, the slides were placed in 10 mM citrate buffer solution (pH 6.0), blocked with 10% normal goat serum for 1 h at room temperature, and then incubated overnight at 4 °C with a primary antibody or an equivalent amount of normal goat IgG as a negative control. Immunoreaction complexes were detected using the avidin–biotin affinity system (Santa Cruz Biotechnology, Santa Cruz, CA), and visualized with 3,3′-diaminobenzidine tetrahydrochloride (Zymed Laboratories, San Francisco, CA) as a chromogen. The sections were counterstained with Mayer's hematoxylin and examined under a light microscope (Cho et al., 2007).

2.7. Microarray

To investigate the change of gene expression by TNP, microarray analysis was performed with total RNA extracted in lung tissue of mouse which was sacrificed at 14 days after a single instillation of TNP 20 mg/kg, using Applied Biosystems Mouse Genome Survey Arrays (Macrogen, Seoul, Korea). Briefly, digoxigenin-11-UTP labeled cRNA was generated and linearly amplified from 1 μg of total RNA purified from control and TNP instillated group, respectively, using Applied Biosystems Chemiluminescent RT-IVT Labeling Kit. Array hybridization, chemiluminescence detection, image acquisition and analysis were performed using Applied Biosystems Chemiluminescence Detection Kit and Applied Biosystems 1700 Chemiluminescent Microarray Analyzer following manufacturer's protocol. Each image was collected for each microarray using the 1700 analyzer which is equipped with high-resolution, large-format CCD camera for gene expression analysis. Images were auto-gridded and the chemiluminescent signals were quantified, corrected for background and spot, and spatially normalized.

2.8. Statistical analysis

The results obtained from the TNP-treated groups were compared to those of the control group. The values were compared using the Student's *t*-test, and significance was represented for each result.

3. Results

3.1. Biochemical analysis of blood

As shown in Table 1, there are no differences between control group and treated group in liver toxicity-related parameters (albumin, AST, ALT, and r-GTP), or in kidney toxicity-related parameters (BUN and creatinine).

3.2. Cytokines in BAL fluid

To identify inflammatory responses induced by TNP instillation, the concentrations of pro-inflammatory cytokines (IL-1, IL-6, and TNF-α), Th1-type cytokines (IL-12 and IFN-γ), and Th2-type cytokines (IL-4, IL-5, and IL-10) were measured in BAL fluid. A significant increase in pro-inflammatory cytokines was observed in BAL fluid after a single intratracheal instillation of TNP (5, 20, 50 mg/kg). Level of IL-6 which plays an important role in the acute inflammation was also increased by TNP treatment. The increased level of IL-6 in the 20 mg/kg TNP-treated group was 433.5 pg/ml, 167 fold higher than that of control group at day 1 after instillation (Table 2). In general, the activated macrophages secrete IL-12 or IL-10 to allow differentiation of naïve CD4 T cells into Th1 or Th2 cells, respectively. In the current study, IL-12 level was 14.5 pg/ml in the control group and this level was significantly elevated in a dose-dependent manner in the TNP-treated groups. In the case of IL-10 which a Th2-type cytokine, the level in the control group was 45.8 pg/ml, while the induced level of 20 mg/kg TNP-treated group, was 142.1 pg/ml. Th1 cells also secrete IFN-γ, which in turn stimulates the Th1 cells themselves and inhibits the activation of Th2 cells. In this study, IFN-γ level was 0.5 pg/ml in control group and was increased to 22.0 pg/ml in the 20 mg/kg TNP-treated group.

Both IL-6 and IL-10 reached their highest levels at day 1 after a single instillation of 20 mg/kg TNP, then decreased over the remainder of the experimental period until day 14. However, IL-4 and IL-2 seemed to be increased in a time-dependent manner till the end of experimental period (Fig. 2).

3.3. Cytokines in the blood

As shown in Table 3, levels of TNF-α, IL-6, IL-10, and IL-12 were significantly increased by a single intratracheal instillation of TNP (5, 20, and 50 mg/kg). IL-6 was increased from 3.6 pg/ml (control group) to 29.8 pg/ml (20 mg/kg TNP-treated group). IL-10 was increased from 48.4 pg/ml of control group to 351.1 pg/ml of 50 mg/kg TNP-treated group, and IL-12 was increased from 56.0 pg/ml of control group to 80.1 pg/ml of 20 mg/kg TNP-treated group.

Table 1
Effects of TNP on serum biochemical parameters. Results were obtained from pooling serum from five mice. TP; total protein, ALB; albumin, AST; aspartate aminotransferase, ALT; alanine aminotransferase, ALP; alkaline phosphatase, r-GT; r-glutamyl transferase, BUN; blood urea nitrogen, Chol; cholesterol.

		TP (g/dL)	ALB (g/dL)	AST (U/L)	ALT (U/L)	ALP (U/L)	r-GTP (U/L)	Creatinine (mg/dL)	BUN (mg/dL)	Chol (mg/dL)
	Control	5.5	3.2	72.5	41.0	132.0	0.0	0.1	14.6	160.5
Day 1	5 mg	5.1	2.9	115.0	59.0	133.0	0.0	0.1	12.3	147.0
	20 mg	5.9	3.4	73.0	53.5	133.5	0.7	0.1	14.8	162.5
	50 mg	5.7	3.3	92.0	51.0	137.0	0.0	0.1	14.9	151.0
20 mg/kg	3 day	5.6	2.9	77.0	66.0	113.0	1.6	0.1	12.9	166.0
	7 day	5.3	3.0	107.0	67.0	137.0	0.1	0.1	14.1	151.0
	14 day	5.7	3.0	87.0	56.0	111.0	0.0	0.1	14.2	174.0

Table 2
Dose-dependent induction of cytokines in BAL fluid of TNP-treated mice.

	Pro-inflammatory			Th1-type		Th2-type		
	IL-1	TNF-α	IL-6	IL-12	IFN-γ	IL-10	IL-4	IL-5
Control	2.6 ± 0.1	4.8 ± 2.1	2.6 ± 0.4	14.5 ± 0.8	0.5 ± 0.1	45.8 ± 5.1	2.5 ± 1.5	2.7 ± 0.4
5 mg/kg	14.2 ± 2.3	34.6 ± 1.1	27.2 ± 1.1	112.9 ± 3.4	2.4 ± 2.1	120.1 ± 2.1	19.4 ± 1.4	7.9 ± 0.2
20 mg/kg	25.9 ± 1.3	144.2 ± 4.2	433.5 ± 5.6	221.7 ± 10.6	22.0 ± 1.1	142.1 ± 6.3	31.0 ± 3.0	10. 5 ± 1. 5
50 mg/kg	26.7 ± 1.3	126.6 ± 2.1	281.8 ± 2.2	145.8 ± 4.8	13.9 ± 3.3	150.6 ± 0.5	36.3 ± 0.7	13.3 ± 1.2

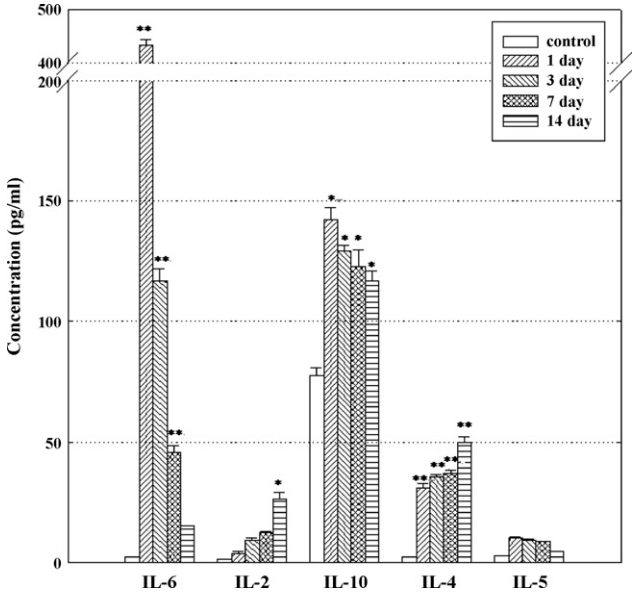

Fig. 2. Time-dependent changes in cytokine levels in BAL fluid after a single intratracheal instillation of TNP. The concentrations of cytokines in BAL fluid harvested on the respective sacrifice days after instillation (TNP 20 mg/kg) were measured using commercially available ELISA kits. Significantly different from control group: $^{*}P < 0.05$; $^{**}P < 0.01$.

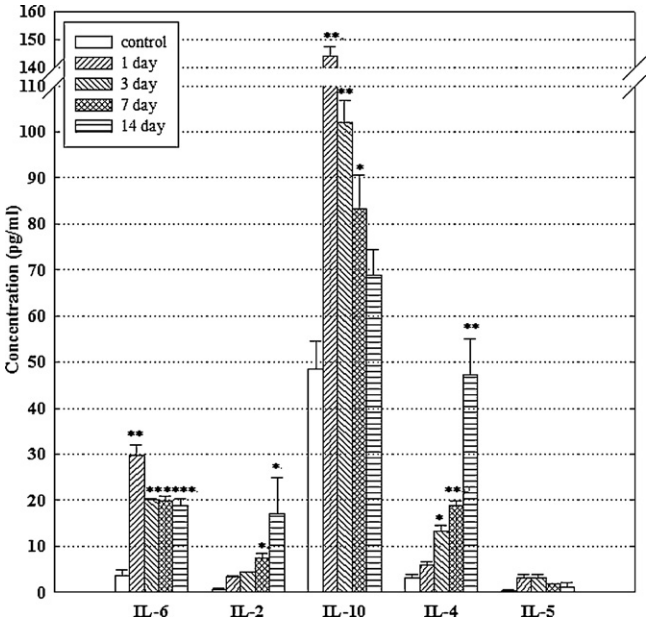

Fig. 3. Time-dependent changes in cytokine levels in blood after a single intratracheal instillation of TNP. The concentrations of cytokines in blood harvested at the respective sacrifice days after instillation (TNP 20 mg/kg) were measured using commercially available ELISA kits. Significantly different from control group: $^{*}P < 0.05$; $^{**}P < 0.01$.

Both IL-6 and IL-10 reached their highest levels at day 1 after a single instillation of TNP 20 mg/kg, then decreased over the remainder of the experimental period until day 14. However, IL-4 and IL-2 seemed to be increased in a time-dependent manner till the end of experimental period (Fig. 3). Time-course of cytokine induction was very similar to those of BAL fluid.

3.4. Lymphocyte phenotypes

Distribution of the lymphocytes was determined in the blood and in spleen of the mice treated with 20 mg/kg TNP at 14 days after instillation. Blood lymphocyte distribution in control group was as follows: 15.29 (NK cell), 42.50% (B cell), and 32.69% (T cell). In TNP-treated group, distribution was changed: 11.09% (NK cell), 58.50% (B cell), and 26.80% (T cell). In the spleen, composition percentages of NK, B and T cell were 3.37%, 69.84%, and 26.11%, respectively in control group. With treatment of 20 mg/kg TNP, the composition percentages were changed to 4.03% (NK cell), 73.84% (B cell), and 21.05% (T cell), respectively. Both in blood and in spleen, B cell proliferation was observed by TNP treatment (Fig. 4). The ratio of $CD4^{+}$ T cells to $CD8^{+}$ T cells, which are the subtype of T cells, was changed from 4.8 in control group to 3.5 at day 14 after instillation (Fig. 5).

3.5. IgE secretion

IgE concentrations in BAL fluid and in blood were measured after the examination of B cell proliferation. As shown in Fig. 6, IgE levels were significantly increased by a single intratracheal instillation of TNP 20 mg/kg both in BAL fluid and in blood and the increased levels were maintained during the experimental period after instillation. At the end of observation day, IgE level reached to 15.0 fold of non-treated control level in BAL fluid and 6.6 fold in the blood, respectively.

Table 3
Dose-dependent induction of cytokines in blood of TNP-treated mice.

	Pro-inflammatory			Th1-Type		Th2-Type		
	IL-1	TNF-α	IL-6	IL-12	IFN-γ	IL-10	IL-4	IL-5
Control	0.0 ± 0.2	2.2 ± 0.1	3.6 ± 0.1	56.0 ± 6.8	0.2 ± 0.1	48.4 ± 2.8	3.1 ± 0.6	0.4 ± 0.4
5 mg/kg	1.8 ± 0.3	2.5 ± 0.9	3.6 ± 0.1	61.2 ± 3.1	1.8 ± 0.5	100.5 ± 4.4	3.4 ± 0.6	1.9 ± 0.2
20 mg/kg	2.2 ± 0.3	8.9 ± 1.1	29.8 ± 1.1	80.1 ± 2.2	2.5 ± 0.2	144.2 ± 4.8	5.8 ± 1.6	3.0 ± 0.1
50 mg/kg	2.9 ± 0.7	6.9 ± 0.1	24.6 ± 1.6	66.3 ± 6.2	1.7 ± 0.5	351.1 ± 17.1	6.9 ± 0.4	4.0 ± 0.3

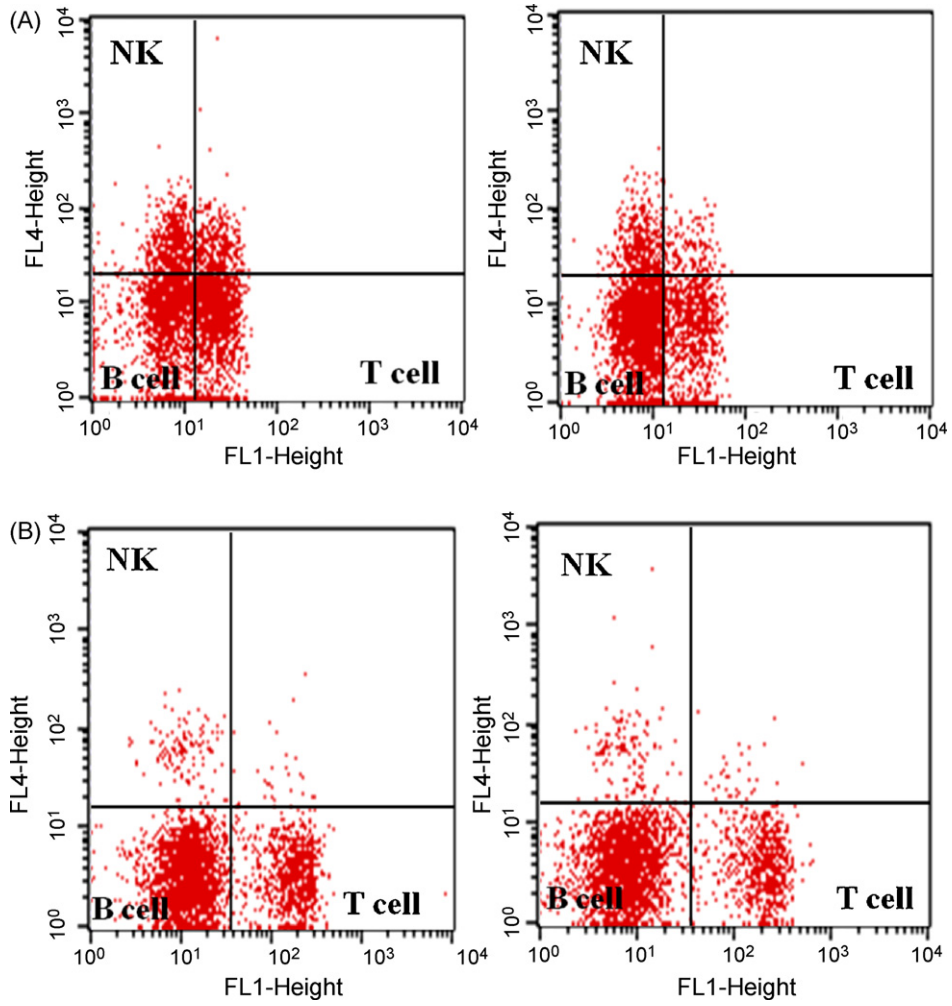

Fig. 4. Analysis of lymphocyte phenotypes in blood and spleen at day 14 after a single intratracheal instillation of TNP. Mice were treated with TNP 20 mg/kg and were sacrificed at day 14 after instillation. All monoclonal antibodies were identified using directly conjugated anti-mouse antibodies, and flow cytometry analysis was performed on the FACSCalibur system. Control samples were matched for each fluorochrome. Distribution of lymphocytes was described in Section 3. (A): blood, (B): spleen.

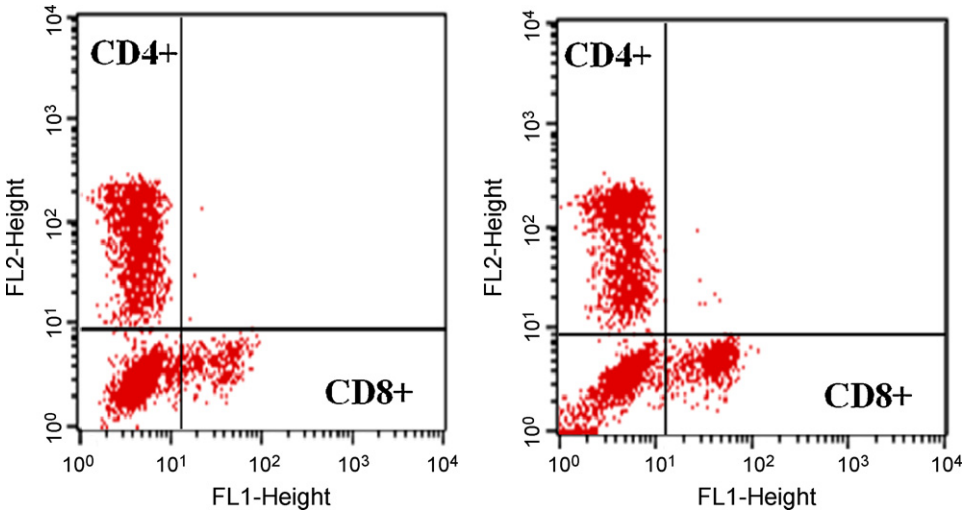

Fig. 5. Analysis of T cell subtypes in blood at day 14 after a single intratracheal instillation of TNP.
Mice were treated with TNP 20 mg/kg and were sacrificed at day 14 after instillation. All monoclonal antibodies were identified using directly conjugated anti-mouse antibodies, and flow cytometry analysis was performed on the FACSCalibur system. Control samples matched for each fluorochrome. Distribution of T cell subtypes was described in Section 3.

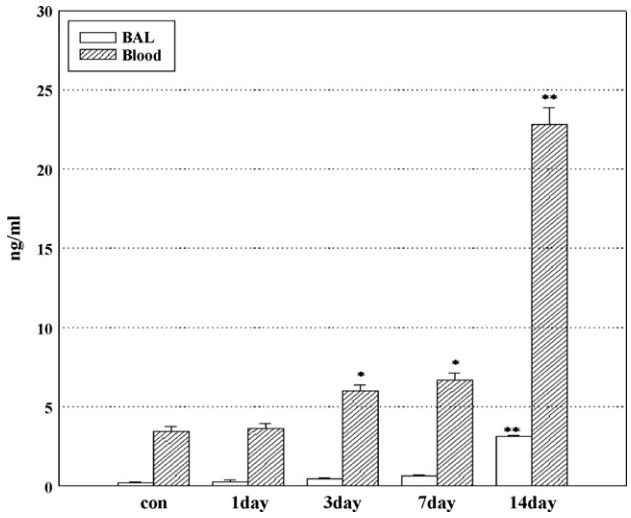

Fig. 6. Levels of IgE in BAL fluid and in blood after a single intratracheal instillation of TNP. Mice were treated with TNP 20 mg/kg and were sacrificed at the designated days after instillation. The concentrations of IgE in BAL fluid and in blood harvested at the respective sacrifice days after instillation were determined using commercially available ELISA kits. Significantly different from control group: $^{*}P < 0.05$; $^{**}P < 0.01$.

3.6. Histopathology and immunohistochemistry

In the lungs, TNP was found throughout the study (14 days) in the bronchiole and alveoli of the lung (Fig. 7). The granulomatous lesions were evident during the experimental period of 14 days after treatment. Increase of MIP-2 (macrophage inflammatory protein-2) was observed at day 1 and MCP-1 (monocyte chemoattractant protein-1) was observed at day 14 (Fig. 8).

3.7. Change of gene expression

Tables 4 and 5 showed up- and down-regulated genes, respectively. 191 genes including H2-T23, Saa3, Slpi, H2-T17, Ccl7, Mmp12, Cxadr, and H2-Eb1 were up-regulated, while 68 genes including Ang4, BC055107, Tnn, Fkbp5, Cidec, and Hbb-b1 were down-regulated. The expressions of genes related with antigen presentation (H2-T23, H2-T17, H2-K1, and H2-Eb1) and genes related with the induction of chemotaxis of immune cells (Ccl7, Ccl3, Cxcl1, Ccl4, Ccl2) were markedly increased. Other inflammation-related genes including Slpi, Saa3, MMP-12, Slc26, Rgs1, and Ctsk were also markedly increased.

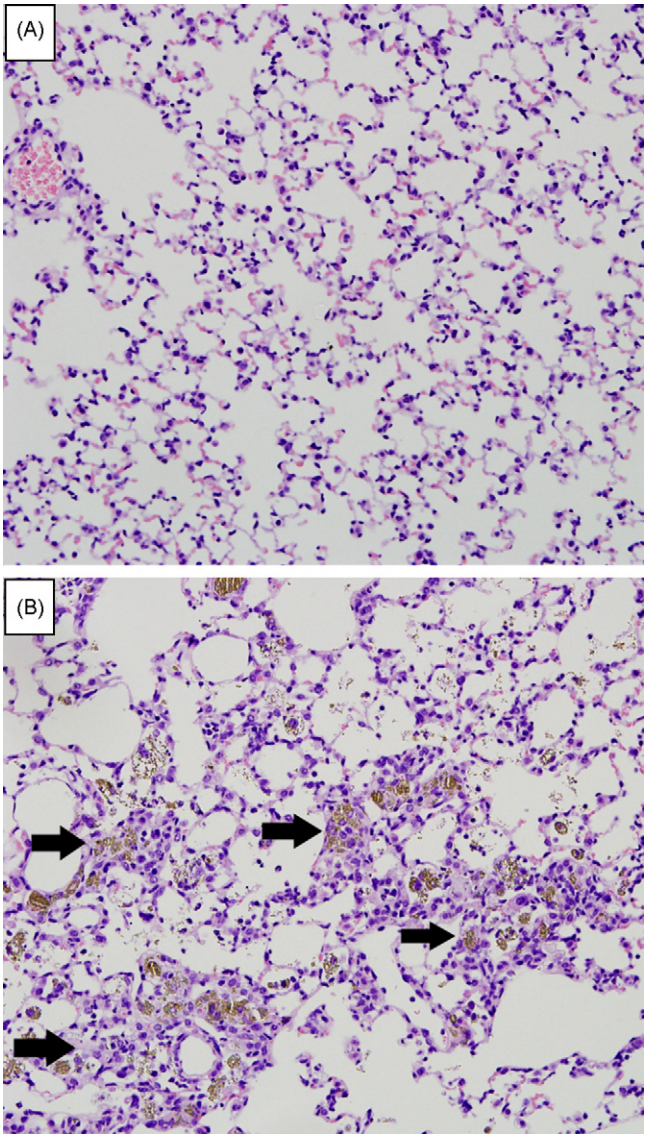

Fig. 7. Histopathological examination of the lungs from mice following the intratracheal instillation of TNP. Mice were treated with TNP 20 mg/kg and were sacrificed on day 14 after instillation. Representative lung sections taken from (A) vehicle control mice, and TNP-treated group at day 14 (B) after instillation. Lung sections were stained with hematoxylin and eosin stains. Black arrows show granulomatous lesions.

4. Discussions

There are many evidences that ambient particulate matters (PM) could act as an trigger of inflammatory diseases such as an adjuvant for allergic sensitization, which raises the possibility that long-term PM exposure may lead to increased prevalence of asthma and skin sensitization (Kleinman et al., 2007; Siegel et al., 2004; Ma and Ma, 2002; Li et al., 2008). However, only a few evidences have been reported that engineered nanoparticles could act as a potential factor for inflammatory diseases. Increased use of engineered nanoparticles including TNP, CNTs, carbon black, and metal nanoparticles in a wide range of industries has introduced a potential new type of inhaled particulate pollutant. It has been known that nanomaterials have special physico-chemical properties and new strategy for toxicity tests and risk assessment of nanomaterials may be introduced.

Recent studies have revealed that exposure to TNP can cause adverse effect to human health through generation of reactive oxygen species (ROS). ROS initiate inflammatory responses and may cause various disease such as emphysema, chronic obstructive lung disease, fibrosis, and lung cancer (Reeves et al., 2008; Kang et al., 2008; Driscoll and Maurer, 1991; Chen et al., 2006). Although the reports on TNP-induced toxicity are now increasing, chronic inflammation-related responses of TNP have not been well studied. In this study, we focused on the cytokine induction, B cell activation, granuloma formation and IgE production by which allergy mechanism or chronic inflammatory disease was induced.

Primary particles of TNP seemed to be agglomerated in the PBS solution (Fig. 1A). Generally, most nanoparticles exist in agglomerated or aggregated form in solution state and TNP in the PBS suspension used for the intratracheal instillation in this study also exist in agglomerated/aggregated form. The mean diameter of the agglomerated particles was about 200 nm (Fig. 1B). As shown in Fig. 1, the size of TNP agglomerates/aggregates was not micrometer level, but nanolevel.

For the acute toxicity of TNP, lethality test and blood biochemical assay were performed. Rats were not killed by TNP in any

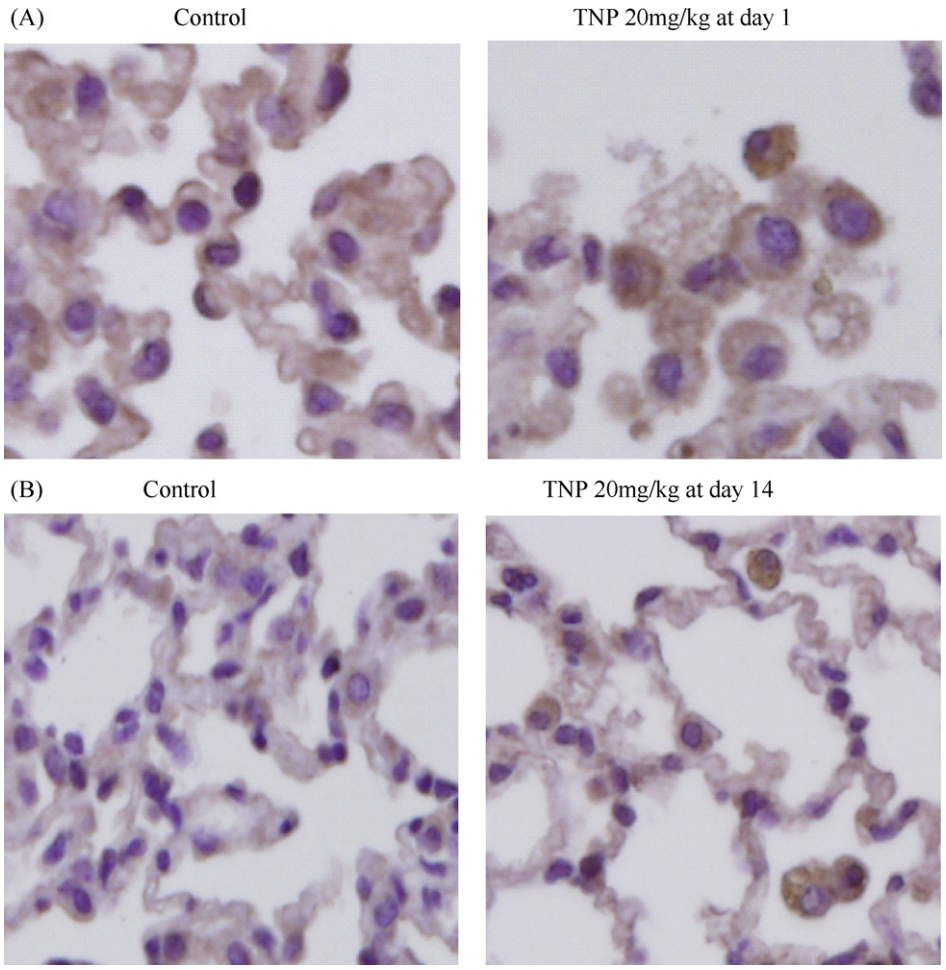

Fig. 8. Immunohistochemical examination of the lungs from mice following the intratracheal instillation of TNP. Mice were treated with TNP 20 mg/kg and were sacrificed at the designated days after instillation. (A) Increased expression of MIP-2 was observed in TNP-treated group at day 1 after instillation. Brown-yellowish color shows the immunoreaction of MIP-2. (B) Increased expression of MCP-1 was observed in TNP-treated group at day 14 after instillation. Brown-yellowish color shows the immunoreaction of MCP-1. Representative lung sections were taken from each group.

treated group, and significant changes in blood biochemistry were not observed (Table 1). Liver function determined by amino transferase activity in serum, and kidney function by BUN or creatinine clearance was not damaged by TNP treatment even in the 50 mg/kg TNP-treated group. Regarding the dosage as nanoparticle-toxicity, the dosage of 50 mg/kg seemed to be high. But it is also important to know the acute adverse effect at higher dosage of nanoparticles for the worst case of exposure. When SWCNTs were intratracheally instilled to rat with 5 mg/kg of high dose, the number of total cells in BAL fluid was not increased (Warheit et al., 2004). It was reported that BAL levels of TNF-α was significantly increased in rat treated with high dose of MWCNTs 2 mg/animal (Muller et al., 2005).

Macrophages which engulfed TNP stimulate inactive T cells by secret cytokines such as IL-1β, TNF-α, and IL-6. Then the activated T cells were differentiated into helper T cells ($CD4^+$) and cytotoxic T cells ($CD8^+$). Furthermore, helper T cells ($CD4^+$) were differentiated into Th1 cell and Th2 cell. In this process, IL-4, IL-5 and IL-10 drive helper T cell to differentiate into Th2 cell that is associated with allergic, or autoimmune responses. The activated Th2 cells may activate B cells to produce IgE. In this study, IL-4 and IL-5 of Th2-type cytokines were increased to 14.4 fold and 4.9 fold of the control level in BAL fluid at day 1 after instillation, respectively.

Although both Th2-type cytokines and Th-1 cytokines were simultaneously increased, Th2 cells are the most effective activators of B cells, especially in primary responses, whereas Th1 cells are crucial for activating macrophages and they are for delayed type hypersensitivity. However, under many circumstances *in vivo*, there are mixed Th1 and Th2 responses, and the overall effects are determined by the dominant responses.

In this study, IL-1, TNF-α, and IL-6 were increased to 9.8 fold, 29.99 fold, and 170.01 fold in the BAL fluid of mouse which was sacrificed at 1 day after instillation with 20 mg/kg, respectively. IL-10 and IL-12 also were increased to 3.1 fold and 15.27 fold of control, respectively. Furthermore, IFN-γ which is a product of Th1 cells was increased to 47.9. IL-4 and IL-5 which are the important component of Th2-mediated response were increased to 12.3, and 3.8 fold of the non-treated control level at 1 day after exposure with 20 mg/kg, respectively (Table 2). IL-10 considered as a Th2-type cytokine may control chronic inflammation and thus the subsequent fibrotic process. Furthermore, activated Th2 cells secret IL-4 which stimulates B cells to produce IgE. IL-2 drives T cell proliferation, NK cell and B cell activation. In this study, while IL-10 reached to maximum at 1 day after exposure, IL-2 and IL-4 were increased in a time-dependent manner until the remainder of experimental period for 14 days after exposure in BAL fluid (Fig. 2). This successive activation of cytokine release was also observed in the blood (Table 3 and Fig. 3). Regarding dose–response, it seemed that the induction of cytokiens by TNP reached plateu at 20 mg/kg and the induction was not further increased. As shown in Tables 2 and 3, induction level of cytokines declined in 50 mg/kg TNP-treated group. It seemed that high dose of 50 mg/kg TNP may exert cytotoxicity to the cytokine-releasing cells.

Table 4
Partial list of genes which were significantly up-regulated in lung at day 14 after a single intratracheal instillatin of TNP 20 mg/kg.

Symbol	Definition	Accession	1st	2nd
H2-T23	Histocompatibility 2, T region locus 23	NM_010398	73.66	113.54
Saa3	Serum amyloid a 3	NM_011315	37.46	47.69
Slpi	Secretory leukocyte peptidase inhibitor	NM_011414	56.40	47.29
H2-T17	Mouse MHC class I H2-TL-T17-c	NM_010396	25.68	30.98
Ccl7	Chemokine (C-C motif) ligand 7 (Ccl7)	NM_013654	11.07	27.25
Mmp12	Mus musculus matrix metallopeptidase 12	NM_008605	16.09	25.88
Cxadr	Mus musculus coxsackie virus and adenovirus receptor	NM_009988	15.89	24.77
H2-Eb1	Mus musculus histocompatibility 2, class II antigen E beta	NM_010382	4.47	23.85
Slc26a4	Solute carrier family 26, member 4	NM_011867	10.24	21.96
H2-K1	Histocompatibility 2, K1, K region	NM_001001892	5.78	21.88
Hal	histidine ammonia lyase	NM_010401	7.31	18.46
LOC100034251	Predicted gene, OTTMUSG00000000971	NM_001081957	5.52	17.42
Gpnmb	Glycoprotein (transmembrane) nmb	NM_053110	2.97	17.38
Ccl3	Mus musculus chemokine (C-C motif) ligand 3	NM_011337	6.01	15.27
Ms4a7	membrane-spanning 4-domains, subfamily A, member 7	NM_027836	5.32	12.28
Cxcl1	chemokine (C-X-C motif) ligand 1	NM_008176	7.06	10.28
Rgs1	Mus musculus regulator of G-protein signaling 1	NM_015811	2.98	10.13
Il4i1	Interleukin 4 induced 1	NM_010215	4.58	9.74
Gpnmb	Glycoprotein (transmembrane) nmb	NM_053110	4.81	9.58
Trem2	triggering receptor expressed on myeloid cells 2	NM_031254	5.01	9.03
2610305D13Rik	RIKEN cDNA 2610305D13 gene	NM_145078	5.12	9.02
Ccl4	Mus musculus chemokine (C-C motif) ligand 4	NM_013652	11.21	8.75
Ccl2	Mus musculus chemokine (C-C motif) ligand 2	NM_011333	3.33	8.48
Spp1	Secreted phosphoprotein 1.	NM_009263	4.13	7.87
Dmkn	Dermokine, transcript variant 2,	NM_172899	5.21	7.17
H2-T23	Histocompatibility 2, T region locus 23	NM_010398	6.34	7.09
AA467197	expressed sequence AA467197	NM_001004174	4.26	7.04
Fcgr2b	Mus musculus Fc receptor, IgG, low affinity IIb	NM_010187	3.05	6.38
Zranb3	Mus musculus zinc finger, RAN-binding domain containing 3	XM_129483	3.73	6.37
Rgs1	Mus musculus regulator of G-protein signaling 1	NM_015811	2.02	6.30
Ctsk	Cathepsin K	NM_007802	5.40	6.24
Noxo1	NADPH oxidase organizer 1	NM_027988	5.27	6.18
Gpnmb	Glycoprotein (transmembrane) nmb	NM_053110	2.79	6.15
Itih4	Inter alpha-trypsin inhibitor, heavy chain 4	NM_018746	3.84	6.13
H2-Bf	Complement factor B	NM_008198	7.05	6.03
Npy	Neuropeptide Y	NM_023456	2.88	6.01
Dmkn	Dermokine (Dmkn), transcript variant 2	NM_172899	4.92	6.00
Mmp13	Matrix metallopeptidase 13	NM_008607	2.19	5.88

Distribution of B cells was increased during the experimental period and peaked at day 14 both in blood and in splenocytes with the induction of Th2-type cytokines (Fig. 4). The activation of B cells induced IgE production both in the blood and in BAL fluid. The level of IgE in blood reached to 6.55 fold of non-treated control level at day 14 after instillation (Fig. 6). Regarding the subtypes of T cells, activated macrophages stimulated naive T cells to trigger adaptive immune system. T cells can be subdivided into two populations according to their expression of $CD4^+$ or $CD8^+$ molecules. In normal human peripheral blood, the contribution ratio of $CD4^+$ T cells and $CD8^+$ T cells is approximately 2:1, but it may be significantly altered by immunodeficiency diseases, autoimmune diseases, and other disorders. In this study, the distribution ratio of $CD4^+$ T cells and $CD8^+$ T cells in non-treated mice was 4.8 but changed to 3.5 in 20 mg/kg TNP-treated group. It means that some inflammation-related response was triggered by TNP. Subtype of T cell, $CD8^+$ cells plays a role in cytotoxicity of infected cells and was activated by MCH I.

Granuloma formation shown in chronic inflammatory disease was also induced in a time-dependent manner in this study (Fig. 7). Treatment of TNP induced acute inflammation at 1 day after instillation. However, chronic inflammation recruited by alveolar macrophages was induced on day 14 after instillation. In addition, nanoparticles damaged the type I epithelial cells. In consequence, the type II epithelial cells were proliferated. Moreover, the lymphocytes were infiltrated in the alveolar regions. The chronic inflammation was gradually increased by the time (data not shown). These results were well correlated with the persistent presence of TNP.

Microarray assay was performed to investigate the regulation of genes related with the previously observed inflammatory responses by TNP in this study. Many MHC class I genes such as H2-T23, H2-T17, H2-K1 were listed as highly up-regulated genes while only a few MHC class II genes (H2-EB1) were listed. This result related with the increased distribution of $CD8^+$ which is activated by MHC class I (Fig. 5). It has been reported that MHC I genes are significantly induced in autoimmune disease and MHC II genes are responsible in allergic responses (Fukami et al., 2009). It has been reported that long-term exposure to certain environmental factors such as heavy metals can activate B cells and IgE production to produce autoimmunity (Abedi-Valugerdi, 2009). Considering the activation of MHC class I gene and autoimmunity, long-term exposure of TNP may be one potential factor for autoimmunity. Genes of Slpi, Saa3, MMP-12, Slc26, Rgs1, and Ctsk were also markedly increased. According to the previous reports, Slpi (secretory leukoprotease inhibitor) was known to be significantly increased in patients with lung carcinoma, acute respiratory distress syndrome, and bronchopulmonary dysplasia (Nukiwa et al., 2008; Ameshima et al., 2000; Sallenave et al., 1999; Watterberg et al., 1994). Gene of saa3 (serum amyloid a3) was listed as the pivotal marker in inflammation including bronchial asthma and in lung cancer (Dai et al., 2007; Jousilahti et al., 2002). Also, MMP-12 (matrix metallopeptidase-2) is believed to be involved in many inflammatory diseases including chronic obstructive pulmonary disease, rheumatoid arthritis and multiple sclerosis (Gossas and Danielson, 2006; Snider, 2003; Liu et al., 2004; Rosenberg, 2002).

In summary, TNP induced pro-inflammatory cytokines, Th1-type cytokines and Th2-type cytokines followed by B cell

Table 5
Partial list of genes which were significantly down-regulated in lung at day 14 after a single intratracheal instillatin of TNP 20 mg/kg.

Symbol	Definition	Accession	1st	2nd
Hbb-b1	Hemoglobin, beta adult major chain	NM_008220	−7.03	−6.36
Bex2	Mus musculus brain expressed X-linked 2	NM_009749	−5.30	−5.07
Twistnb	Mus musculus TWIST neighbor	NM_172253	−5.14	−3.63
Bex2	Brain expressed X-linked 2	NM_009749	−4.94	−5.48
Tnn	Tenascin N	NM_177839	−4.47	−6.50
9030612M13Rik	Mus musculus RIKEN cDNA 9030612M13 gene	NM_172458	−4.35	−3.91
Fkbp5	FK506 binding protein 5	NM_010220	−4.12	−6.48
Efhd1	Mus musculus EF hand domain containing 1	NM_028889	−4.06	−4.08
1200009F10Rik	Mus musculus RIKEN cDNA 1200009F10 gene	NM_026166	−3.40	−3.50
MGC29978	Mus musculus acetyl-Coenzyme A acyltransferase 1B	NM_146230	−3.38	−5.01
2610511O17Rik	Tetratricopeptide repeat domain 27	NM_152817	−3.37	−3.75
Agtr1a	Angiotensin II receptor, type 1a	NM_177322	−3.31	−2.54
Angptl4	Mus musculus angiopoietin-like 4	NM_020581	−3.13	−3.53
Cdh13	Mus musculus cadherin 13	NM_019707	−3.12	−2.74
BC055107	Mus musculus family with sequence similarity 107	NM_183187	−3.11	−7.08
Mbd1	Methyl-CpG binding domain protein 1	NM_013594	−3.05	−2.79
Akr1e1	Mus musculus aldo-keto reductase family 1, member E1	NM_018859	−3.05	−3.71
Map3k6	Mitogen-activated protein kinase kinase kinase 6	NM_016693	−3.00	−5.55
BC049975		XM_138237	−2.99	−3.39
Ang4	Angiogenin, ribonuclease A family, member 4	NM_177544	−2.98	−13.78
Mbd1	methyl-CpG binding domain protein 1	NM_013594	−2.87	−2.33
LOC228862		XM_130649	−2.77	−3.35
Bex4	Brain expressed gene 4	NM_212457	−2.74	−2.36
Retnlg	Resistin like gamma	NM_181596	−2.73	−3.00
Bex4	Brain expressed gene 4	NM_212457	−2.73	−2.19
Lims2	LIM and senescent cell antigen like domains 2	NM_144862	−2.69	−2.70
Pcolce2	Mus musculus procollagen C-endopeptidase enhancer 2	NM_029620	−2.69	−2.46
Npr3	Natriuretic peptide receptor 3, transcript variant 1	NM_008728	−2.68	−4.36
3632451O06Rik	Mus musculus RIKEN cDNA 3632451O06 gene	NM_026142	−2.68	−3.24
Twistnb	Mus musculus TWIST neighbor	NM_172253	−2.65	−2.35
Cidec	cell death-inducing DFFA-like effector c	NM_178373	−2.65	−6.44
Spon2	Spondin 2, extracellular matrix protein	NM_133903	−2.61	−2.73
Ramp3	Receptor (calcitonin) activity modifying protein 3	NM_019511	−2.56	−2.36
Lmcd1	LIM and cysteine-rich domains 1	NM_144799	−2.55	−2.59
Ppp1r1b	Protein phosphatase 1, regulatory (inhibitor) subunit 1B	NM_144828	−2.54	−2.91
Chia	Chitinase, acidic	NM_023186	−2.52	−3.64
Gap43	Mus musculus growth associated protein 43	NM_008083	−2.52	−2.19
6720430O15	Tetraspanin 18	NM_183180	−2.50	−2.63
Srp9	Signal recognition particle 9	NM_012058	−2.48	−2.08
Prkag3	Mus musculus protein kinase, AMP-activated, gamma 3 non-catatlytic subunit	NM_153745	−2.45	−2.20

proliferation. IgE production was also increased both in BAL fluid and in the blood. Granuloma formation and the expressions of pro-inflammatory proteins (MIP and MCP) were observed in lung tissue. Furthermore, many genes related with MHC class I were over-expressed in lung tissue by a single instillation of TNP. This result suggested TNP may be one of triggers to be responsible for chronic inflammation and autoimmunity.

Conflict of Interest

None.

Acknowledgements

This work was supported by Ministry of Environment Eco-technopia 21 project and by National Institute of Environmental Research.

Appendix A. Supplementary data

Supplementary data associated with this article can be found, in the online version, at doi:10.1016/j.tox.2009.03.005.

References

Abedi-Valugerdi, M., 2009. Mercury and silver induce B cell activation and anti-nucleolar autoantibody production in outbred mouse stocks: are environmental factors more important than the susceptibility genes in connection with autoimmunity? Clin. Exp. Immunol. 155 (1), 117–124.

Alberg, T., Cassee, F.R., Groeng, E.C., Dybing, E., Løvik, M., 2009. Fine ambient particles from various sites in europe exerted a greater IgE adjuvant effect than coarse ambient particles in a mouse model. J. Toxicol. Environ. Health A. 72 (1), 1–13.

Ameshima, S., Ishizaki, T., Demura, Y., Imamura, Y., Miyamori, I., Mitsuhashi, H., 2000. Increased secretory leukoprotease inhibitor in patients with nonsmall cel lung carcinoma. Cancer 89 (7), 1448–1456.

Byun, J.A., Ryu, M.H., Lee, J.K., 2006. The immunomodulatory effects of 3-monochloro-1,2-propanediol on murine splenocyte and peritoneal macrophage function in vitro. Toxicol. In Vitro 20 (3), 272–278.

Chen, H.W., Su, S.F., Chien, C.T., Lin, W.H., Yu, S.L., Chou, C.C., Chen, J.J., Yang, P.C., 2006. Titanium dioxide nanoparticles induce emphysema-like lung injury in mice. FASEB J. 20 (13), E1732–E1741.

Cho, W.S., Choi, M., Han, B.S., Cho, M., Oh, J., Park, K., Kim, S.J., Kim, S.H., Jeong, J., 2007. Inflammatory mediators induced by intratracheal instillation of ultrafine amorphous silica particles. Toxicol. Lett. 175, 24–33.

Dai, S., Wang, X., Liu, L., Liu, J., Wu, S., Huang, L., Xiao, X., He, D., 2007. Discovery and identification of serum amyloid a protein elevated in lung cancer serum. Sci. China C Life Sci. 50 (3), 305–311.

Driscoll, K.E., Maurer, J.K., 1991. Cytokine and growth factor release by alveolar macrophages: potential biomarkers of pulmonary toxicity. Toxicol. Pathol. 19 (4), 398–405.

Fukami, N., Ramachandran, S., Saini, D., Walter, M., Chapman, W., Patterson, G.A., Mohanakumar, T., 2009. Antibodies to MHC class I induce autoimmunity: role in the pathogenesis of chronic rejection. J. Immunol. 182 (1), 309–318.

Gossas, T., Danielson, U.H., 2006. Characterization of Ca^{2+} interactions with matrix metallopeptidase-12: implications for matrix metallopeptidase regulation. Biochem. J. 398 (3), 393–398.

Grassian, V.H., O'Shaughnessy, P.T., Adamcakova-Dodd, A., Pettibone, J.M., Thorne, P.S., 2007. Inhalation exposure study of titanium dioxide nanoparticles with a primary particle size of 2 to 5 nm. Env. Health Perspect. 115 (3), 397–402.

Gurr, J.R., Wang, A.S., Chen, C.H., Jan, K.Y., 2005. Ultrafine titanium dioxide particles in the absence of photoactivation can induce oxidative damage to human bronchial epithelial cells. Toxicology 213 (1–2), 66–73.

Haar, C., Hassing, I., Bol, M., Bleumink, R., Pieters, R., 2006. Ultrafine but not fine particulate matter causes airway inflammation and allergic airway sensitization to co-administered antigen in mice. Clin. Exp. Allergy 36 (11), 1469–1479.

Jousilahti, P., Salomaa, V., Hakala, K., Rasi, V., Vahtera, E., Palosuo, T., 2002. The association of sensitive systemic inflammation markers with bronchial asthma. Ann. Allergy Asthma Immunol. 89 (4), 381–385.

Kang, S.J., Kim, B.M., Lee, Y.J., Chung, H.W., 2008. Titanium dioxide nanoparticles trigger p53-mediated damage response in peripheral blood lymphocytes. Environ. Mol. Mutagen. 49 (5), 399–405.

Kleinman, M.T., Sioutas, C., Froines, J.R., Fanning, E., Hamade, A., Mendez, L., Meacher, D., Oldham, M., 2007. Inhalation of concentrated ambient particulate matter near a heavily trafficked road stimulates antigen-induced airway responses in mice. Inhal. Toxicol. 19, 117–126.

Lee, K.P., Trochimowicz, H.J., Reinhardt, C.F., 1985. Pulmonary response of rats exposed to titanium dioxide (TiO_2) by inhalation for two years. Toxicol. Appl. Pharmacol. 79 (2), 179–192.

Li, N., Nei, A.E., 2008. The role of oxidative stress in ambient particulate matter-induced lung diseases and its implications in the toxicity of engineered nanoparticles. Free Radic. Biol. Med. 44 (9), 1689–1699.

Liu, M., Sun, H., Wang, X., Koike, T., Mishima, H., Ikeda, K., Watanabe, T., Ochiai, N., Fan, J., 2004. Association of increased expression of macrophage elastase(matrix metalloproteinase 12) with rheumatoid arthritis. Arthritis Rheum. 50 (10), 3112–3117.

Ma, J.Y., Ma, J.K., 2002. The dual effect of the particulate and organic components of diesel exhaust particles on the alteration of pulmonary immune/inflammatory responses and metabolic enzymes. J. Environ. Sci. Health C Environ. Carcinog. Ecotoxicol. Rev. 20 (2), 117–147.

Manosroi, A., Saraphanchotiwitthaya, A., Manosroi, J., 2005. In vitro immunomodulatory effect of Pouteria cambodiana(Pierre ex Dubard) Baehni extract. J. Ethnopharmacol. 101 (1–3), 90–94.

Muller, J., Huaux, F., Moreau, N., Misson, P., Heilier, J.F., Delos, M., Arras, M., Fonseca, A., Nagy, J.B., Lison, D., 2005. Respiratory toxicity of multi-wall carbon nanotubes. Toxicol. Appl. Pharmacol. 207 (3), 221–231.

Nukiwa, T., Suzuki, T., Fukuhara, T., Kikuchi, T., 2008. Secretory leukocyte peptidase inhibitor and lung cancer. Cancer Sci. 99 (5), 849–855.

Oberdörster, G., Oberdörster, E., Oberdörster, J., 2005. Nanotoxicology: an emerging discipline evolving from studies of ultrafine particles. Environ. Health Perspect. 113 (7), 823–839.

Ohrui, T., Zayasu, K., Sato, E., Matsui, T., Sekizawa, K., Sasaki, H., 2000. Pulmonary tuberculosis and serum IgE. Clin. Exp. Immunol. 122 (1), 13–15.

Park, E., Yi, J., Chung, K., Ryu, D., Choi, J., Park, K., 2008. Oxidative stress and apoptosis induced by titanium dioxide nanoparticles in cultured BEAS-2B cells. Toxicol. Lett. 180, 222–229.

Rahman, Q., Lohani, M., Dopp, E., Pemsel, H., Jonas, L., Weiss, D.G., Schiffmann, D., 2002. Evidence that ultrafine titanium dioxide induces micronuclei and apoptosis in Syrian hamster embryo fibroblasts. Environ. Health Perspect. 110 (8), 797–800.

Reeves, J.F., Davies, S.J., Dodd, N.J.F., Jha, A.N., 2008. Hydroxyl radicals(*OH) are associated with titanium dioxide(TiO2) nanoparticle-induced cytotoxicity and oxidative DNA damage in fish cells. Mutat. Res. 640, 113–122.

Rosenberg, G.A., 2002. Matrix metalloproteinases and neuroinflammation in multiple sclerosis. Neuroscientist 8 (6), 586–595.

Sallenave, J.M., Donnelly, S.C., Grant, I.S., Robertson, C., Gauldie, J., Haslett, C., 1999. Secretory leukocyte proteinase inhibitor is preferentially increased in patients with acute respiratory distress syndrome. Eur. Respir. J. 13 (5), 1029–1036.

Siegel, P.D., Saxena, R.K., Saxena, Q.B., Ma, J.K., Ma, J.Y., Yin, X.J., Castranova, V., Al-Humadi, N., Lewis, D.M., 2004. Effect of diesel exhaust particulate(DEP) on immune responses: contributions of particulate versus organic soluble components. J. Toxicol. Environ. Health A 67 (3), 221–231.

Silva, I.A., Graber, J., Nyland, J.F., Silbergeld, E.K., 2005. In vitro HgCl2 exposure of immune cells at different stages of maturation: effects on phenotype and function. Environ. Res. 98, 341–348.

Snider, G.L., 2003. Understanding inflammation in chronic obstructive pulmonary disease: the process begins. Am. J. Respir. Crit. Care Med. 167 (8), 1045–1046.

Vendrame, M., Gemma, C., Pennypacker, K.R., Bickford, P.C., Davis, Sanberg, C., Sanberg, P.R., Willing, A.E., 2006. Cord blood rescues stroke-induced changes in splenocyte phenotype and function. Exp. Neurol. 199, 191–200.

Warheit, D.B., Laurence, B.R., Reed, K.L., Roach, D.H., Reynolds, G.A., Webb, T.R., 2004. Comparative pulmonary toxicity assessment of single-wall carbon nanotubes in rats. Toxicol. Sci. 77 (1), 117–125.

Warheit, D.B., Borm, P.J., Hennes, C., Lademann, J., 2007. Testing strateges to establish the safety of nanomaterials: conclusion of an ECETOC workshop. Inhal. Toxicol. 19 (8), 631–643.

Watterberg, K.L., Carmichael, D.F., Gerdes, J.S., Werner, S., Backstrom, C., Murphy, S., 1994. Secretory leukocyte protease inhibitor and lung inflammation in developing bronchopulmonary dysplasia. J. Pediatr. 125 (2), 264–269.

Yamadori, I., Ohsumi, S., Taguchi, K., 1986. Titanium dioxide deposition and adenocarcinoma of the lung. Acta Pathol. Jpn. 36 (5), 783–790.